

IRES-based Vector Coexpressing FGF2 and Cyr61 Provides Synergistic and Safe Therapeutics of Lower Limb Ischemia

Audrey Rayssac^{1,2}, Charles Neveu¹⁻³, Mélanie Pucelle^{1,2}, Loïc Van den Berghe^{1,2}, Leonel Prado-Lourenco^{1,2,4}, Jean-François Arnal¹⁻³, Xavier Chaufour¹⁻³ and Anne-Catherine Prats^{1,2}

¹Inserm, U858, Toulouse, France; ²Université de Toulouse, UPS, Institut de Médecine Moléculaire de Rangueil, IFR150, Toulouse, France;

³Centre Hospitalier Universitaire de Toulouse, Toulouse, France; ⁴Millegen, Prologue 1–La Pyrénéenne, BP 2701, Labège, France

Due to the lack of an adequate conventional therapy against lower limb ischemia, gene transfer for therapeutic angiogenesis is seen as an attractive alternative. However, the possibility of side effects, due to the expression of large amounts of angiogenic factors, justifies the design of devices that express synergistic molecules in low controlled doses. We have developed an internal ribosome entry site (IRES)-based bicistronic vector expressing two angiogenic molecules, fibroblast growth factor 2 (FGF2), and Cyr61. Through electrotransfer into the ApoE^{-/-} mice hindlimb ischemic muscle model, we show that the IRES-based vector gives more stable expression than either monocistronic plasmid. Furthermore, laser Doppler analysis, arteriography, and immunohistochemistry clearly show that the bicistronic vector promotes a more abundant and functional revascularization than the monocistronic vectors, despite the fact that the bicistronic system produces 5–10 times less of each angiogenic molecule. Furthermore, although the monocistronic Cyr61 vector accelerates B16 melanoma growth in mice, the bicistronic vector is devoid of such side effects. Our results show an active cooperation of FGF2 and Cyr61 in therapeutic angiogenesis of hindlimb ischemia, and validate the use of IRES-based bicistronic vectors for the coexpression of controlled low doses of therapeutic molecules, providing perspectives for a safer gene therapy of lower limb ischemia.

Received 22 April 2009; accepted 13 August 2009; published online 8 September 2009. doi:10.1038/mt.2009.211

INTRODUCTION

Lower limb arterial disease is a pathology with a prevalence of about 12% (ref. 1). Critical limb ischemia, which has a high prevalence in diabetic patients, affects about 500 new individuals/million/year in the United States and Europe. Even with medical treatments, such as arterial angioplasty and arterial bypass,

only 25% of limbs can be salvaged. More than 50% of patients die within 5 years, despite amputation of necrosed limbs, and their quality of life is deplorable.

In this context, therapeutic angiogenesis, which aims to restore tissue perfusion in response to angiogenic growth factors, represents a promising alternative. The principle of therapeutic angiogenesis is to administer angiogenic regulators that stimulate the establishment of a stable, functional vascular network. Several major angiogenic growth factors, such as vascular angiogenic growth factor, fibroblast growth factor 1 (FGF1), and fibroblast growth factor 2 (FGF2), as well as other angiogenic molecules have been assayed in several preclinical and clinical studies employing protein or gene therapy.^{2,3} Although protein therapy is inconvenient due to the short half-life of therapeutic molecules, gene therapy permits the sustained production of angiogenic factors and results in prolonged exposure to the therapeutic molecules. Plasmid-based systems are presently being used in clinical trials of lower limb ischemia.⁴⁻⁶

The current clinical trials are based on the use of a single angiogenic factor, mainly vascular angiogenic growth factor or FGF.^{4,6} However, the formation of a functional vascular network is a complex process that requires several angiogenic factors in order to obtain capillary sprouting as well as induce the growth and remodeling of collateral arteries.⁷

Co-injecting two different therapeutic expression vectors does not ensure that both products will be expressed with the expected ratio, as various events can lead to preferential silencing or removal of one vector.⁸ Combined gene therapy for therapeutic angiogenesis thus necessitates the development of an adequate gene transfer system that allows stable coexpression of both molecules. In this context, the use of internal ribosome entry sites (IRESs) provides an attractive approach to coexpress combinations of molecules. IRESs, RNA structural elements present in the 5' untranslated region of several mRNAs, permit an internal recruitment of the translational machinery. They can be used as biotechnological tools to drive expression of additional genes encoded within a single mRNA.⁹ Thus, IRESs permit the design of expression

C.N. and M.P. contributed equally to this work.

Correspondence: Anne-Catherine Prats, Team "Translational control and gene therapy of vascular and tumoral diseases", Institut National de Santé et de la Recherche Médicale, U858, Institute of Molecular Medicine of Rangueil, IFR150, 1, Avenue Jean Poulhès, BP 84225, 31432 Toulouse Cedex 4, France. E-mail: Anne-Catherine.Prats@inserm.fr

cassette coding for combinations of therapeutic molecules on the same transcription unit. Furthermore, IRESs may be tissue and/or context specific. In particular, we have previously shown that the FGF1 IRES is very active in skeletal muscle and capable of being used in gene transfer vectors targeted to ischemic limbs.^{8,10}

In the present study, we have designed an IRES-based, bicistronic vector in order to optimize therapeutic angiogenesis in the mouse ApoE^{-/-} model of hindlimb ischemia.¹¹ FGF2 and Cyr61 were chosen as angiogenic molecules, as both have been reported as therapeutic candidates.^{3,12} Cyr61 (also known as CCN1) belongs to the CCN (cyr61, ctgf, and nov) family, matri-cellular regulatory factors involved in internal and external cell signaling. Recently characterized as an angiogenic factor, Cyr61 is a heparin-binding, extracellular matrix-associated protein that mediates endothelial cell adhesion and migration by binding to integrin $\alpha2\beta3$ (ref. 13). Cyr61 plays a role in both physiological and pathological angiogenesis.¹³ In addition, Cyr61 has been described for its ability to enhance FGF2-induced DNA synthesis in endothelial cells.¹³⁻¹⁵ We compared mono- and bicistronic vectors expressing FGF2 and/or Cyr61 after intramuscular administration of naked DNA. Their efficacy was evaluated in an ischemia leg model and their safety was tested in a heterotopic tumor model.

RESULTS

IRES-based bicistronic vectors generate lower amounts of FGF2 and Cyr61 than monocistronic vectors

In order to test the potential synergism of FGF2 and Cyr61 in the promotion of therapeutic angiogenesis, an IRES-based bicistronic vector was generated. We used the FGF1 IRES, previously shown to be the most efficient for gene transfer in skeletal muscle.^{8,10} The complementary DNAs coding Cyr61 or FGF2 were subcloned into monocistronic and bicistronic vectors (Figure 1a; pC-FGFiCyr, pC-Cyr, and pC-FGF, respectively).

Bicistronic control vectors were also constructed: pC-FGFiL codes for FGF2 and firefly luciferase (Luc F), whereas pC-RiCyr codes for Renilla luciferase (Luc R) and Cyr61. These two vectors, which express a single angiogenic molecule in the bicistronic context, permit the evaluation of the effects of FGF2 or Cyr expressed individually but at similar doses to those obtained with the FGF-Cyr vector pC-FGFiCyr. Indeed, monocistronic vectors are expected to generate higher amounts of molecules of interest than their bicistronic counterparts.⁸ The bicistronic vector pC-RiL serves as a negative control that produces Luc R and Luc F. Efficient expression of FGF2 and/or Cyr61 by the different plasmids was checked by transient transfection of COS-7 cells. As expected, the bicistronic vectors expressed lower amounts of both angiogenic factors than the monocistronic vectors (Supplementary Figure S1).

The different plasmids were electrotransferred in tibialis anterior muscle of ApoE^{-/-} mice with the expression of FGF2 and Cyr61 followed by western blot analysis. A semiquantitative analysis of vector expression was performed by serial dilution of the samples (Figure 1b,c). For both FGF2 and Cyr61, the monocistronic vectors were highly expressed, but decreased 30-fold between day 7 and day 21. In contrast, bicistronic vector expression decreased only three- to fivefold during the same time period. Because the two vectors are expressed with a similar efficiency at day 21, we can deduce that day 7 bicistronic expression is about 5–10 times less efficient than the monocistronic vector, but that the bicistronic vector delivers more stable expression over time.

The different vectors were then electrotransferred into the ischemic muscles of mice submitted to surgery (see Materials and Methods). Expression of the two angiogenic factors was followed between day 7 and day 21 (Supplementary Figure S2a,b). The Cyr61/FGF2 detected in the control transfectants (pC-RiL) corresponds to endogenous protein. In nonoperated mice,

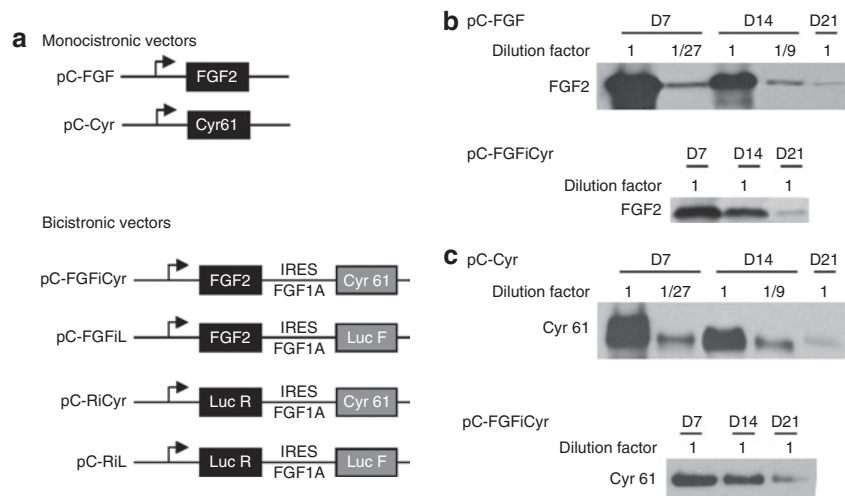


Figure 1 Monocistronic and bicistronic vector construction and expression in mouse tibialis anterior muscle. **(a)** Schematics of monocistronic and bicistronic vectors. The monocistronic plasmids encode either human FGF2 or human Cyr 61 under the control of the cytomegalovirus (CMV) promoter. Bicistronic vectors contain two genes separated by the FGF1 IRES A.²⁴ The first gene is FGF2 or *Renilla* luciferase (Luc R). The second gene is Cyr 61 or firefly luciferase (Luc F). These plasmids have the same skeleton as the monocistronic vectors (see **Supplementary Materials and Methods**). **(b,c)** Semiquantitative analysis of FGF2 and Cyr61 expression. Following electrotransfer in tibialis anterior of monocistronic or bicistronic plasmids pC-FGF, pC-Cyr, or pC-FGFiCyr (50 µg each), muscle extracts (serial dilution by 1/3, 1/9, and 1/27 for the monocistronic vectors) were analyzed 7, 14, or 21 days after electrotransfer, by western blot using anti-FGF2 **(b)** or anti-Cyr61 **(c)** antibodies (see **Supplementary Materials and Methods**).

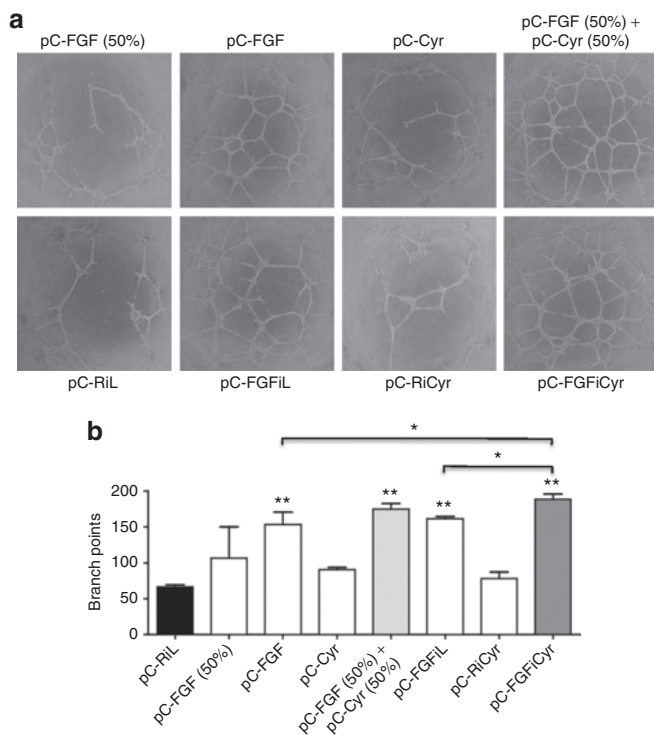


Figure 2 Effect of Cyr61 and FGF2 on endothelial cell tubulogenesis *in vitro*. **(a)** Representative photographs of adult bovine aortic endothelial cells plated on Matrigel-coated wells in the presence of cell-conditioned media (60 μ l), a mix of pC-FGF (30 μ l) and pC-Cyr (30 μ l) conditioned media [called pC-FGF (50%) + pC-Cyr (50%)], and a mix of pC-FGF (30 μ l) conditioned media and Opti-MEM (30 μ l) (called pC-FGF 50%) after 20 hours. **(b)** Branch points were quantified. The data shown are the mean \pm SEM ($n = 3$ wells per group) (* $P < 0.05$, ** $P < 0.01$ versus control group) of a representative duplicate experiment.

the monocistronic vectors expressed high levels of angiogenic factors at day 7, with a strong decrease in expression at day 21. In contrast, the bicistronic vectors expressed the therapeutic molecules in a less efficient but more stable manner (**Supplementary Figure S2c,d**).

In order to investigate the mechanism that leads to less efficient protein expression with the IRES containing constructs, we transfected C2C12 myoblasts with the different vectors. Protein expression was higher with the monocistronic than with the bicistronic vectors in C2C12, as observed in muscle (**Supplementary Figure S3a,b**). However, the mRNA amount quantified by reverse transcription and quantitative PCR using either FGF2 or Cyr61 primers, revealed similar amounts of mono- and bicistronic mRNAs, suggesting that their different protein expression results from a translational process (**Supplementary Figure S3c,d**).

FGF2 and Cyr61 cooperate to stimulate angiogenesis *in vitro*

Cyr61 has been shown to mediate enhancement of FGF2-induced DNA synthesis in human umbilical vein endothelial cells.¹⁵ This prompted us to evaluate a possible cooperative effect of both angiogenic factors on angiogenesis *in vitro*. Conditioned media, obtained from 293 cells transfected by the monocistronic or bicistronic vectors containing FGF2, Cyr61 or both, were used

to treat adult bovine aortic endothelial cells plated on Matrigel (**Figure 2**). Angiogenesis was assessed by quantification of the branch points, showing that FGF2 is more angiogenic than Cyr61, *in vitro* (**Figure 2a,b**). However, conditioned medium from cells transfected with the bicistronic vector FGF-Cyr was slightly, but significantly more efficient at stimulating angiogenesis than conditioned media containing FGF2 alone, suggesting a cooperation of the two angiogenic factors.

The FGF-Cyr bicistronic vector generates efficient blood perfusion and reduced necrosis and inflammation with low doses of angiogenic factors

In order to test the effect of the therapeutic vectors on revascularization of ischemic tissues, we used the hindlimb ischemia model described previously.¹¹ Surgery was performed on hypercholesterolemic ApoE^{-/-} mice, which have been shown to exhibit delayed skeletal muscle healing after hindlimb ischemia-reperfusion.¹⁶ Naked DNA was electrotransferred just following surgery, and the effect of the different vectors on tissue reperfusion was measured by laser Doppler imaging (**Figure 3a,b**). Data showed that the monocistronic as well as the bicistronic vectors expressing FGF2 and/or Cyr61 were able to improve limb reperfusion from day 7 after treatment, with an optimal effect at day 14 (**Figure 3c**). The effect of the angiogenic vectors decreased at day 21, as a probable result of both lower vector expression and natural revascularization occurring in mice without treatment.

These data show that coexpression of low doses of FGF2 and Cyr61 by the bicistronic vector are able to elicit reperfusion as efficiently as the five- to tenfold higher doses produced by the monocistronic vectors (**Figure 3c,d** compare pC-FGFiCyr with pC-Cyr and pC-FGF). In order to check the hypothesis of a synergy between the two angiogenic factors, we used the control bicistronic vectors expressing FGF2 or Cyr61 alone at low doses (**Figure 3e**, pC-FGFiL and pC-RiCyr). The efficiency of these constructs on reperfusion was less important, suggesting a synergistic effect of FGF2 and Cyr61 on revascularization.

The beneficial effect of the angiogenic vectors was also evaluated by determining the degree of ischemia, based on the presence or absence of necrosis, for each individual (**Figure 4**, see Materials and Methods). Coexpression of FGF2 and Cyr61 by the bicistronic vector decreased hindlimb necrosis by 37%, whereas necrosis in the untreated controls was at 85% (**Figure 4**, pC-FGFiCyr). The beneficial effect of the bicistronic vector on necrosis was similar or superior to that of the monocistronic vectors (48 and 39% of necrosed tissue for pC-Cyr and pC-FGF, respectively), confirming the synergistic effect of FGF2 and Cyr61 coexpressed at low doses.

As Cyr61 has been described to promote the inflammation response, the presence of macrophages was analyzed 21 days after surgery/electrotransfer by immunodetection of CD11b. A large number of macrophages were detected in the muscles treated by the control vector pC-RiL indicating strong inflammation (**Figure 4b**). The treatment by either of the angiogenic vectors generated a decrease in macrophage accumulation, even for pC-Cyr, which is less anti-inflammatory than pC-FGF. Interestingly, the bicistronic vector pC-FGFiCyr was the most efficient at accelerating inflammation resolution (**Figure 4b**).

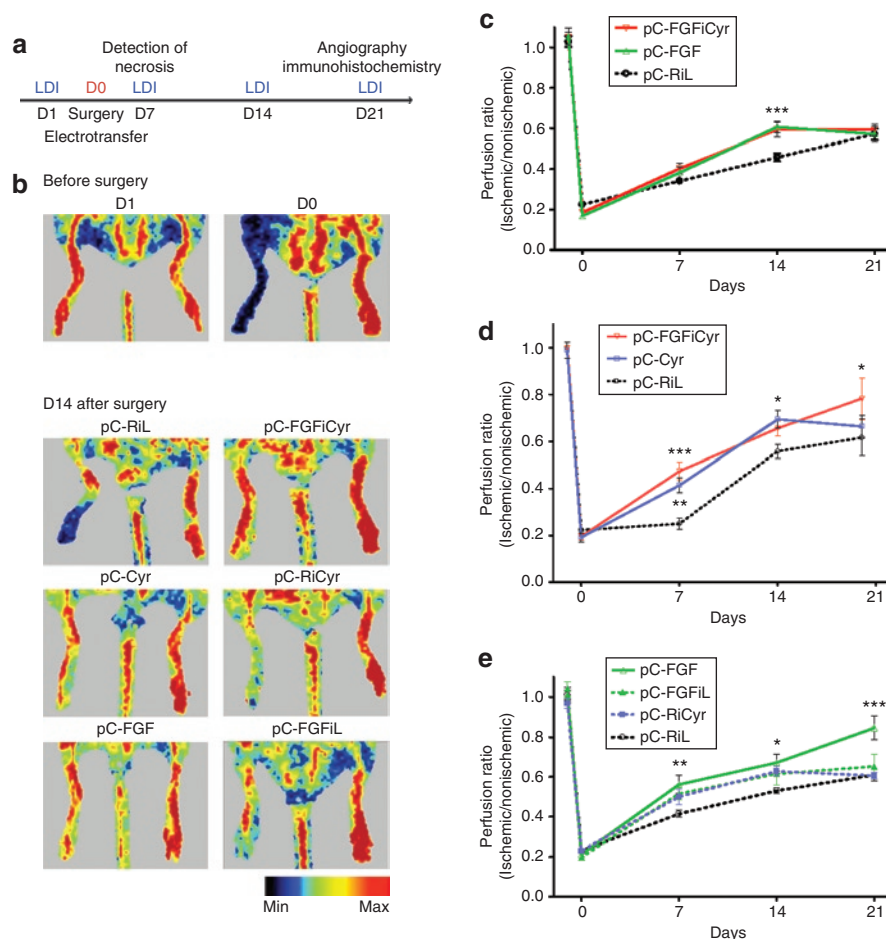


Figure 3 Effect of angiogenic vector treatment on blood flow recovery in the ischemic hindlimb. **(a)** Experimental protocol. The days are indicated (D1–D21) and the dates of laser Doppler imaging (LDI) are indicated. **(b)** Representative LDI before surgery and at day 14 after surgery for each group. A color scale illustrates blood flow variations from minimal (dark blue) to maximal (red) values. Immediately after unilateral femoral artery excision (D0), a marked reduction in blood flow of one hindlimb appears in blue. **(c,d)** Comparison of treatments by the bicistronic vector pC-FGFiCyr or by monocistronic vector pC-FGF or pC-Cyr measured by quantification of LDI ratio (ischemic limb/nonischemic limb) in ApoE^{-/-} mice. LDI was performed preoperatively, postoperatively, and every week until day 21 postoperatively. **(c)** Mice were treated by electrotransfer of either pC-FGFiCyr, pC-FGF or the control pC-RiL. **(d)** Mice were treated by either pC-FGFiCyr, pC-Cyr or the control pC-RiL. **(e)** Comparison of treatments with the bicistronic control vectors expressing FGF2 or Cyr alone (pC-FGFIL and pC-RiCyr) or the monocistronic vector pC-FGF. Mice were treated by electrotransfer of either pC-FGFIL, or pC-RiCyr, or pC-FGF, or pC-RiL, and LDI was performed as above. The data are the mean \pm SEM ($n = 7$ animals per group) (* $P < 0.05$, ** $P < 0.01$, *** $P < 0.001$ versus control group). Each experiment was performed in triplicate.

The bicistronic vector enables the synergistic effect of FGF2 and Cyr61 to act on angiogenesis and arteriogenesis in ischemic hindlimb

In order to evaluate more precisely the effect of the bicistronic vector on angiogenesis and arteriogenesis, ischemic hindlimb revascularization was analyzed by angiography and immunohistochemistry.

Angiographic analysis of collateral vessel development in the ischemic leg was investigated 21 days after surgery/transfection (Figure 5a and Supplementary Figure S4). Importantly, quantification of the vascular networks demonstrated that the angiographic score is significantly higher after treatment with bicistronic FGF-Cyr (Figure 5b and Supplementary Figure S4d, pC-FGFiCyr) but not with the other vectors. The bicistronic vector was also the only one to generate a significant increase of vessel length and the number of segments (Figure 5c,d). In addition, bicistronic FGF-Cyr generated the best perfusion of the distal

end of the leg, explained by major arteriogenesis on the thigh (Figure 6).

Capillary density and mature vessel formation were analyzed by immunohistochemistry using antibodies against CD31, α -SMA, or β -dystroglycan to detect endothelial cells, smooth muscle cells, and skeletal muscle fibers, respectively (Figure 7). As expected, the monocistronic vector expressing FGF2, a strong inducer of capillary vessel formation, had a higher effect than the vector expressing Cyr61 (Figure 7b). FGF2 was also more efficient than Cyr61 at inducing the formation of mature vessels (Figure 7c). However, the bicistronic vector coexpressing FGF2 and Cyr61 was able to increase the number of capillaries and mature vessels, related to muscle fibers, more efficiently than the monocistronic vector that expresses higher levels of FGF2. Similar data were obtained when reporting vessel number with respect to the surface area (data not shown).

Taken together, these data show that coexpression of low doses of FGF2 and Cyr61, through the bicistronic vector, is significantly

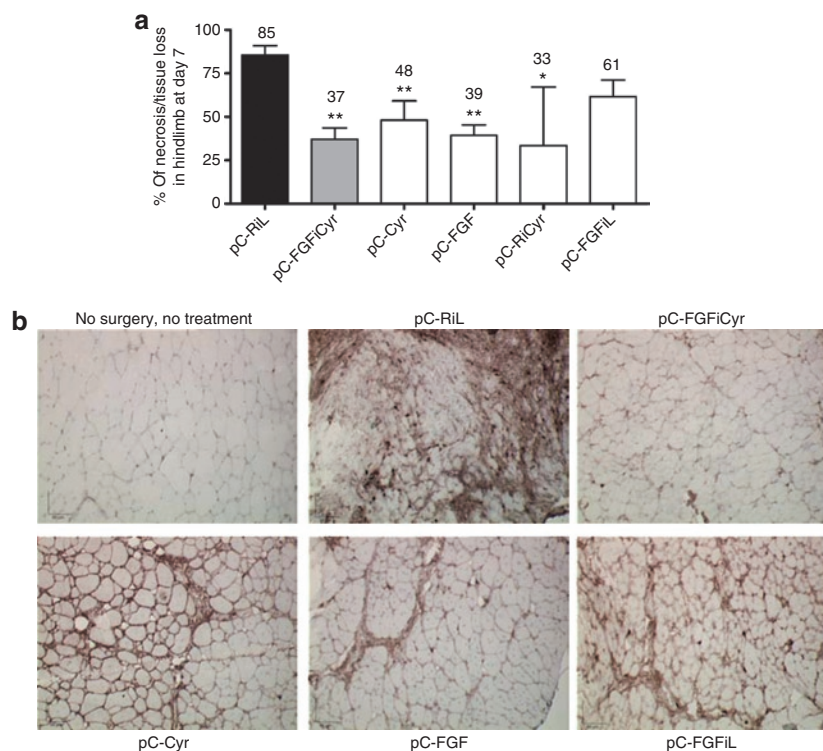


Figure 4 Clinical ischemia index and inflammation. **(a)** The mice were observed for gross changes, and we assessed the degree of necrosis based on the presence or absence of pressure sores, gangrene, or autoamputation. The data are the mean of percent \pm SEM ($n = 7$ animals per group) ($*P < 0.05$, $**P < 0.01$ versus control group). Experiments were performed in triplicate. **(b)** Representative photomicrographs of ischemic tibialis anterior muscles stained with anti-CD11b allowing the detection of macrophages 21 days after surgery and electrotransfer. Original magnification $\times 200$. Bar = 67 μ m.

more efficient than either monocistronic vector on both angiogenesis and arteriogenesis leading to ischemic hindlimb reperfusion.

The bicistronic FGF-Cyr vector, in contrast to the monocistronic vector expressing Cyr61 alone, is devoid of side effects on tumor growth

An important issue in developing a gene therapy treatment is generating a therapeutic vector devoid of undesirable side effects. In particular, FGF2 and Cyr61, as angiogenic factors, may act to enhance tumor progression. For that reason, a vector expressing low doses of such molecules will be safer with respect to their side effects.

The two monocistronic vectors expressing FGF2 or Cyr61, and the bicistronic FGF-Cyr vector were assessed, as well as the control vector coding luciferase genes, for a possible effect on the development of B16 melanoma (**Figure 8**). Results clearly showed no undesirable effects with the bicistronic vector coexpressing FGF2 and Cyr61, whereas the monocistronic vector expressing Cyr61 generated a significant increase in tumor volume and weight (**Figure 8a,b**). As the monocistronic vector expressing FGF2 did not increase tumor volume or weight, this deleterious action appears to be ascribed to high Cyr61 expression.

The effect of vector treatment was also analyzed in the nonischemic legs of the treated mice, revealing no variation of capillary number with any of the therapeutic vectors (**Figure 8c**).

These data indicate that the IRES-based vector, expressing low amounts of synergistic FGF2 and Cyr61, is applicable to a safer and efficient form of gene therapy for hindlimb ischemia.

DISCUSSION

In the present study, we have developed an IRES-based bicistronic vector driving coexpression of two angiogenic molecules, FGF2 and Cyr61. Our data show that FGF2 and Cyr61 have synergistic effects on therapeutic angiogenesis, allowing the bicistronic FGF-Cyr vector to generate the formation of a more abundant and functional vessel network than the monocistronic vectors, despite the fact that the FGF-Cyr vector produces lower amounts of the therapeutic molecules than the monocistronic vectors producing FGF2 or Cyr61 alone. Such a feature of the bicistronic vector is pivotal, as it does not induce negative side effects such as the acceleration of tumor development, observed when Cyr61 is produced in large amounts by the monocistronic vector. These data not only validate the concept of synergism of angiogenic molecules coexpressed by a single gene transfer vector, but also reveal the importance of considering the dose and the ratio of the angiogenic molecules, and not only the efficiency of expression in gene therapy protocols.

The positive effect of synergism between FGF2 and Cyr61 is observed for all parameters of the newly formed collateral vessel network: size, length, and abundance. Furthermore, the amount of capillaries is also significantly increased. Taken together, the data show that association of the two molecules generates a more stable and functional vascular network. The efficiency of a combined treatment to improve therapeutic revascularization has previously been shown by others in ischemic hindlimb models;¹⁷⁻¹⁹ however, we show here a real synergism between FGF2 and Cyr61, as the bicistronic FGF-Cyr vector generates improved therapeutic angiogenesis

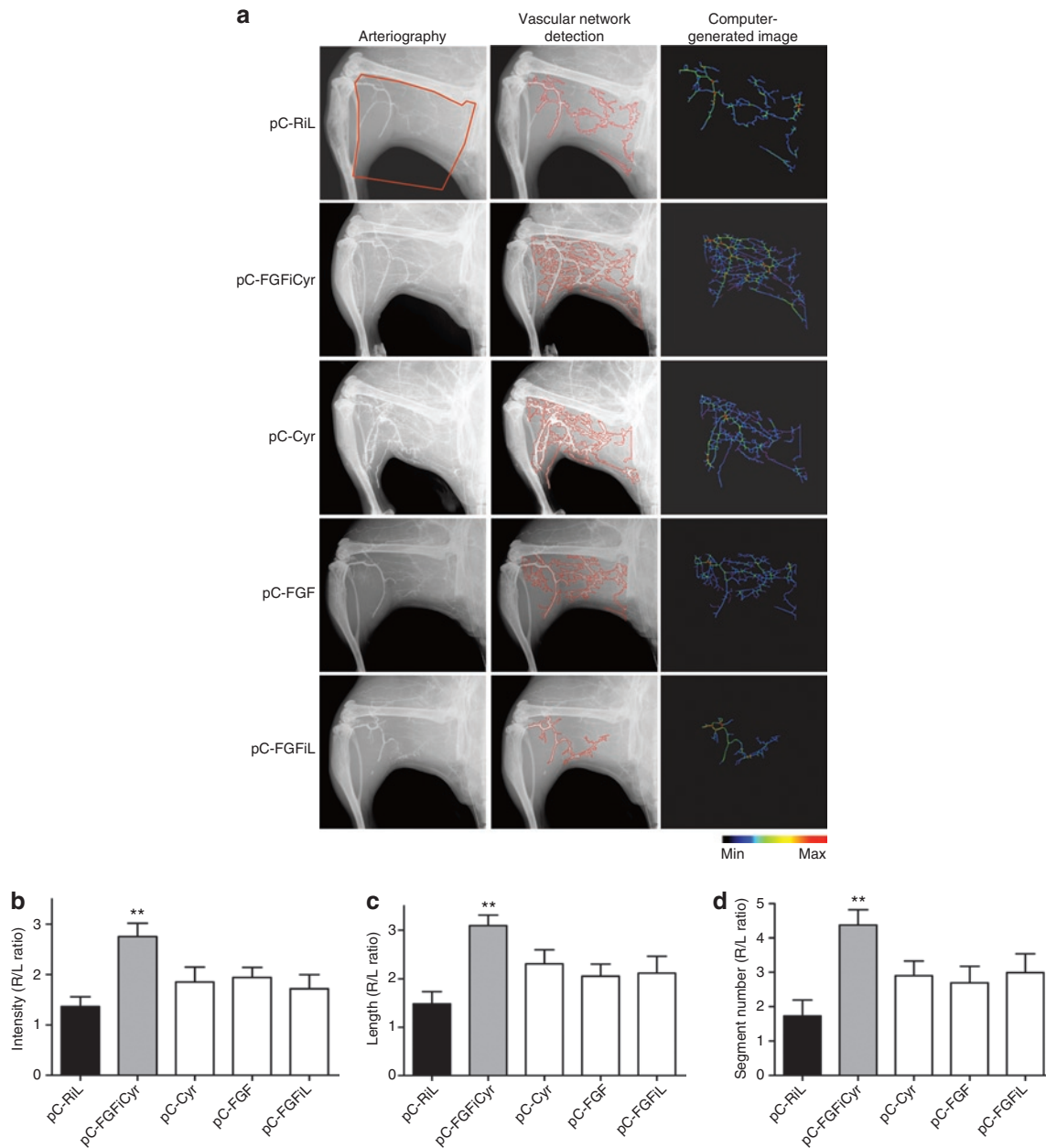


Figure 5 Angiographic analysis of collateral vessel development in the ischemic limb. **(a)** Representative angiograms of collateral vessel formation in ApoE KO C57Bl/6 mice at day 21 after surgery. The area of interest (red zone) was delineated by the position of the ligation on the femoral artery, the knee, the edge of the femur, and external limit of the leg (left column). The image analysis software (Morpho Expert) detected vessel network automatically (middle column) and created computer-generated images (right column) for quantification. A color scale illustrates vessel size variations from thin (dark blue) to large (red) values. **(b–d)** Quantitative analysis of three criteria: angiographic score (vessel area) **(b)**, total length **(c)**, and number of segments **(d)** of collateral vessel network. These criteria were determined by pixel analysis and expressed as the ratio of the ischemic to nonischemic limb (R/L ratio). The data are the mean \pm SEM ($n = 6$ animals per group) (** $P < 0.01$ versus control group).

and arteriogenesis with significantly lower doses of the angiogenic factors. In a previous report, showing the beneficial effects of FGF2 and platelet-derived growth factor association, the same dosage of molecules was administered either alone or together.¹⁷ In other studies using gene transfer, equal amounts of plasmids encoding angiopoietin-1 and vascular angiogenic growth factor were used either alone or together, whereas the authors used a constant amount of total plasmid in the most recent study and reported an improved reperfusion due to vascular angiogenic growth factor and

FGF2 association.^{18,19} The marked difference in the present study is that the doses produced by the bicistronic vector are 5–10 times lower than that obtained with the monocistronic vectors.

An interesting issue is why the bicistronic vectors produce less angiogenic factors than the monocistronic vectors. The lower level but more stable expression concerns not only the second cistron (IRES-driven), but also the first cistron. Analysis of mRNA levels in C2C12 myoblasts suggests that protein expression levels result from a translational event rather than from alterations in mRNA

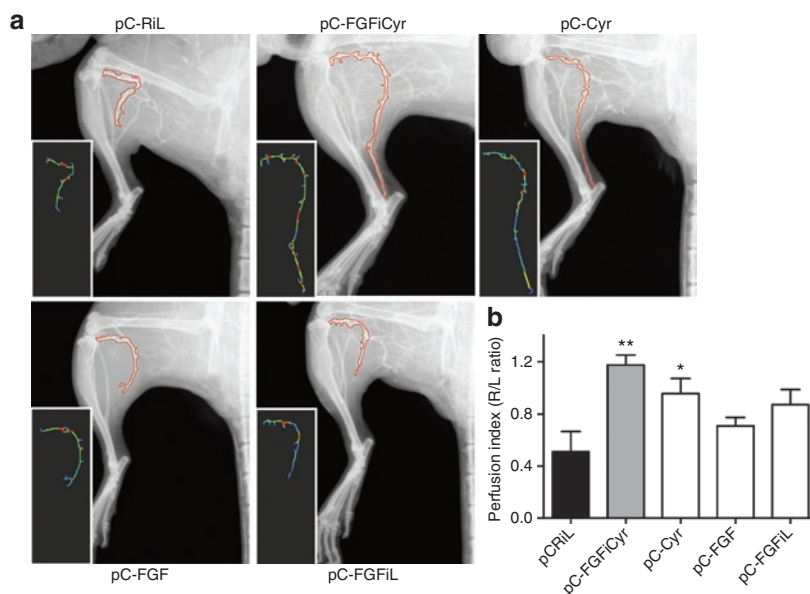


Figure 6 Perfusion index in the ischemic limb. **(a)** Representative selected zone of major vessels of the leg (included popliteal and tibial vessels, from the knee to the foot) **(b)** Calculation of perfusion index of the foot. This criterion was determined by pixel analysis and expressed as the ratio of the length of popliteal and tibial vessels in ischemic versus nonischemic limb (R/L ratio). The data are the mean \pm SEM ($n = 6$ animals per group) (* $P < 0.05$, ** $P < 0.01$ versus control group).

stability. The lower expression may be related to translational features of the FGF1 IRES: it has been previously shown by us and others that the presence of an IRES can influence translation of the first cistron.^{10,20} The mechanism proposed by Jünemann *et al.* from their study using the encephalomyocarditis virus IRES is that whenever the cap-binding complex eIF-4F has been captured to a bicistronic mRNA by binding to a picornavirus IRES via its eIF-4G moiety, it can be provided in *cis* to the 5' end of the mRNA and stimulate translation initiation. In contrast, the present study shows an inhibitory effect of the IRES on translation of both cistrons. We can hypothesize that the IRES could control the recruitment of the bicistronic mRNA into polysomes, a process that might be governed by limiting IRES trans-acting factors, resulting in the translational control of both cistrons. Lower expression could also limit the elimination of the vector by the mouse immune system and result in a more stable long-term expression.

The more efficient long-term expression shown here is consistent with our previous data demonstrating that IRESs allow expression of a stable ratio of the two molecules of interest.⁸ Thus, prolonged expression and stable ratio represent two factors that could favor the establishment of a stable and functional vessel network. In particular, the ratio may be important for maintaining the synergistic effect of the angiogenic molecules.

The FGF1 IRES used in this study is of cellular origin. This is the first time, to our knowledge, that a cellular IRES has been used in a vector expressing therapeutic molecules in a disease model. The FGF1 IRES has been chosen due to its efficiency in skeletal muscle and because its physiological properties are expected to be closer to endogenous genes than the encephalomyocarditis virus IRES classically used in bicistronic vectors. Also, the FGF1 IRES, at least in an adeno-associated virus vector context, allows optimal vector expression when compared to a similar vector with the encephalomyocarditis virus IRES.¹⁰ Furthermore, we have

previously shown that IRESs from angiogenic factor mRNAs, but not the encephalomyocarditis virus IRES, are activated in ischemic and hypoxic conditions.^{21,22} This has been confirmed in the present study. Such a controlled activation allowing a significant but limited expression of the transgenes may be a crucial feature of the FGF1 IRES containing vector.

The main mechanism described for the synergy between FGF2 and Cyr61 is that Cyr61, having a high affinity with heparan sulfate proteoglycan, is able to specifically displace FGF2 from the extracellular matrix.¹⁵ Coexpression of low amounts of Cyr61 could thus displace the endogenous FGF2 bound to the extracellular matrix and also prevent sequestration of the FGF2 produced by the vector in the extracellular matrix, resulting in an efficient diffusion of FGF2 throughout the entire limb. Indeed, larger amounts of diffusible FGF2 were detected in serum with the bicistronic vector (data not shown). This could explain the increased distant arteriogenic effect of FGF2 in the thigh, when coexpressed with Cyr61. However, our data also indicate that Cyr61, especially when expressed in large amounts, shows intrinsic effects that are more likely related to its binding to specific receptors rather than to FGF2 displacement. Indeed, overexpression of Cyr61, but not FGF2, is able to accelerate the B16 melanoma tumor progression in mouse. This underlines the interest of using a vector generating low amounts of Cyr61, not only for its beneficial local synergistic effect with FGF2 but also to avoid systemic undesirable effects on tumor growth and potentially other actions such as aggravation of diabetic retinopathy.

We show that, in this given experimental model, the dose of bicistronic plasmid used (50 μ g/mouse) elicits a very favorable benefit to risk ratio (*i.e.*, therapeutic angiogenesis versus harmful tumor growth). The absence of undesirable effects on tumor growth is reassuring in the perspective of clinical studies. However, dose-response should be established in a human clinical trial,

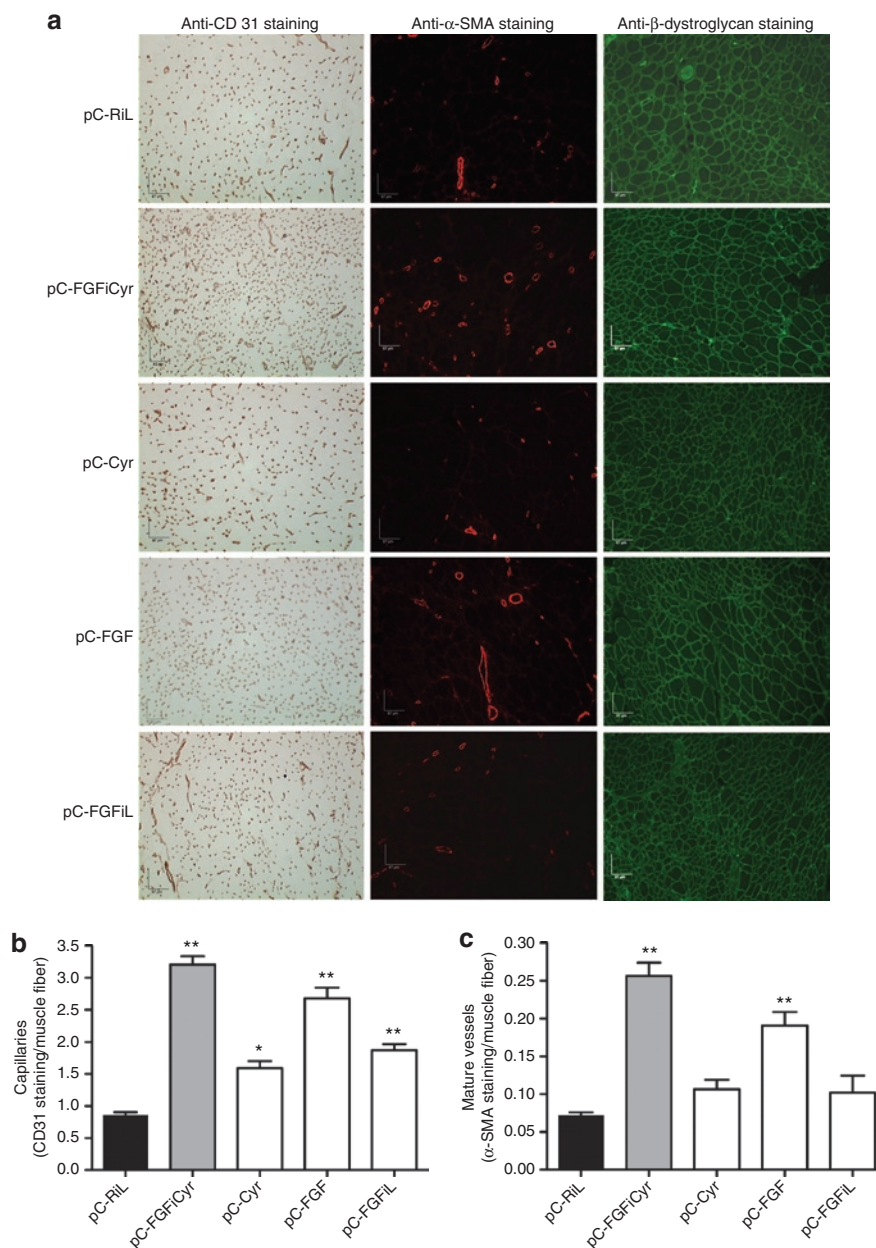


Figure 7 Analysis of capillary density and mature vessel formation. **(a)** Representative photomicrographs of ischemic tibialis anterior muscles stained with antibodies against CD31, α -SMA, or β -dystroglycan, allowing the detection of capillaries, mature vessels, or muscle fibers, respectively, 21 days after surgery and electrotransfer. Original magnification $\times 200$. Bar = 67 μ m. **(b)** Quantification of capillary density in ischemic tibialis anterior muscle of treated (with pC-FGF1Cyr, pC-Cyr, pC-FGF, or pC-FGFIL) or untreated (with pC-RiL) mice using anti-CD 31 antibody and reported to the number of muscle fibers. Data are expressed as the mean \pm SEM ($n = 6$) (* $P < 0.05$, ** $P < 0.01$ versus control group). **(c)** Quantification of mature vascular density in ischemic tibialis anterior muscle of treated (with pC-FGF1Cyr, pC-Cyr, pC-FGF, or pC-FGFIL) or untreated (with pC-RiL) mice, using anti- α -SMA antibody and reported to the number of muscle fibers. Data are expressed as the mean \pm SEM ($n = 6$) (** $P < 0.01$ versus control group).

in particular because the profound histological alterations that characterize the critical lower limb ischemia could alter transfection efficiency and vector expression.

These data provide important perspectives for gene therapy of lower limb ischemia. The FGF1 IRES-based vector constitutes an attractive tool to control both the long-term expression as well as establish a low dose and ratio of coexpressed angiogenic factors. Furthermore, this system offers the possibility to add a third, or even a fourth angiogenic factor to increase the synergy and obtain

a functional vessel network with still lower doses of the angiogenic factors, thus diminishing again the risk of side effects and providing optimized angiogenic vector candidates for clinical trials of lower limb ischemia.

MATERIALS AND METHODS

Hindlimb ischemia mouse model. Animal experiments were conducted in accordance with recommendations of the European Convention for the Protection of Vertebrate Animals used for experimentation.

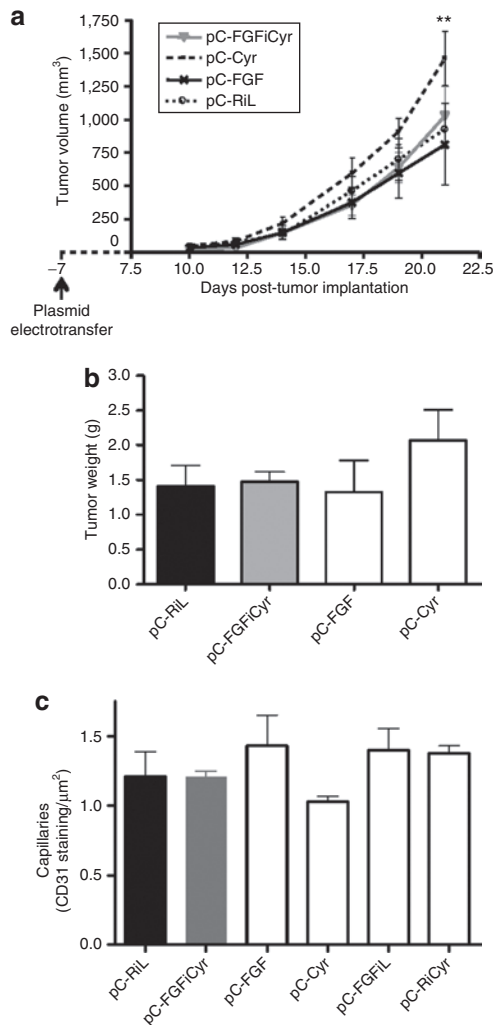


Figure 8 Effects of Cyr 61 and FGF2 expressed via mono- and bicistronic vectors on tumor growth. **(a)** B16F0 cells (250,000 cells) were transplanted subcutaneously in the right flank in C57BL/6 mice divided into four groups ($n = 6$): pC-RiL, pC-FGF, pC-Cyr, and pC-FGF/Cyr (electrotransferred 7 days before B16F0 injections). Tumor growth was monitored three times a week 7 days after B16F0 cell implantation. Each point is the mean \pm SEM of six mice per group. (** $P < 0.01$ versus control group). **(b)** Comparison of the average of subcutaneous tumors by weighing explanted tumors from mice in each group when the tumor burden in treated pC-Cyr mice required euthanasia. Data are the mean weights \pm SEM from six mice per group. Experiments were performed in duplicate. **(c)** Quantification of capillary density in the nonischemic tibialis anterior muscles (left leg) of treated (pC-FGF/Cyr, pC-Cyr, pC-FGF, or pC-FGF/RiL) or untreated (pC-RiL) mice using anti-CD 31 antibody and reported by μm^2 . Data are expressed as the mean \pm SEM ($n = 3$).

Experiments were performed on 12- to 15-week-old female C57BL/6 ApoE^{-/-} mice²³ and on 4-week-old female C57BL/6 mice from Janvier (Le Genest St Isle, France).

Unilateral hindlimb ischemia was created in 12- to 15-week-old female C57BL/6 ApoE^{-/-} mice as described.¹¹ Animals were anesthetized and depilated using depilatory cream (Veet), and then an incision was performed in the skin overlying the middle portion of the right hindlimb. After ligation of the proximal end of the right femoral artery, the distal portion of the saphenous artery was ligated, and the artery and all branches from the inguinal ligament up to and including the saphenous–popliteal bifurcation were dissected free and excised.

For hindlimb ischemia experiments, 12- to 15-week-old female ApoE^{-/-} mice were randomly divided into six groups of six mice each. All mice underwent surgically induced hindlimb ischemia the same day as gene transfer. Mice underwent laser Doppler perfusion imaging before and after gene transfer, and 7, 14, and 21 days after gene delivery. Seven days after surgery and gene transfer, we evaluated the degree of ischemia by limb observation based on the presence or absence of pressure sores, gangrene, or autoamputation (clinical ischemia index). Twenty-one days after surgery, mice underwent angiography and then tibialis anterior muscles were harvested for immunohistological analysis after killing.

Laser Doppler perfusion imaging. Blood flow in both ischemic and nonischemic hindlimbs was measured until day 21 using a PeriScan System blood perfusion monitor laser Doppler equipment (Laser Doppler perfusion imaging system; Perimed, Stockholm, Sweden). Three consecutive measurements were averaged after scanning of the same region of interest (leg and foot) with the laser Doppler perfusion imaging. The perfusion signal was displayed in color codes ranging from dark blue (low or no perfusion) to red (high perfusion). Results are expressed as the ratio of perfusion in the ischemic limb versus nonischemic hindlimb.

Angiography. Angiographic analysis of collateral vessel development in the ischemic limb was performed by angiography on anesthetized animals. After abdominal aorta exposure, a 24G polyethylene catheter (BD, Franklin Lakes, NJ) was used to cannulate the aorta, 5 ml phosphate-buffered saline was injected, followed by 0.5–0.8 ml contrast medium (Micropaque, barium sulfate 1g/ml; Guerbet, Roissy, France).

High-definition angiograms were generated with a Faxitron X-Ray imager (MX-20; Faxitron X-Ray, Lincolnshire, IL) and films exposed 10 seconds 22kV, then numerized for quantitative evaluation using image analysis software Morpho Expert (Explora Nova, La Rochelle, France). Images were examined to identify collateral vessels that bridged the ligated femoral artery. Morpho Expert allowed analysis of three criteria: angiographic score (vessel area), total length, and number of segments of collateral vessel network. These criteria were determined by pixel analysis and expressed as the ratio of the ischemic to nonischemic limb (R/L ratio). The area of interest was delineated by ligature position on the femoral artery, knee, edge of the femur, and leg external limit.

Histological analysis. Muscles were snap-frozen in isopentane cooled in liquid nitrogen and stored at -80°C . Samples were embedded in OCT compound (Tissue-Tek; Sakura Finetek, Torrance, CA) and snap-frozen in liquid nitrogen. A series of $8\mu\text{m}$ transverse frozen-embedded sections cut at $200\mu\text{m}$ intervals over the muscle length were immunostained with specific antibodies. The capillaries were counted after staining with αCD31 antibody (rat monoclonal antibody against mouse CD31, 1:50; BD Biosciences Pharmingen, San Diego, CA). Macrophages were revealed with αCD11b antibody (rat monoclonal antibody against mouse CD11b, 1:20; ref. 550282; BD Biosciences Pharmingen). The avidin–biotin–horseradish peroxidase system (Vector Laboratories, Burlingame, CA) with diaminobenzidine as a chromogen (Dako, Glostrup, Denmark) was used to reveal immunoreactivity. Frozen sections were stained with monoclonal antibodies against α -actin (α -SMA, 1:400, clone 1A4, Cy3 conjugate; Sigma-Aldrich, St Louis, MO) and against human β -dystroglycan (Novocastra, Newcastle upon Tyne, UK), detected by biotinylated antibodies followed by avidin–fluorescein isothiocyanate (M.O.M. kit, Vector Laboratories). Immunopositive signals were revealed using a fluorescein isothiocyanate–conjugated secondary and Cy3-conjugated streptavidin, and examined under a fluorescent microscope (Nikon, Melville, NY) at $\times 200$ magnification. Capillaries, mature vessels, and fibers were automatically counted with Morpho Expert under a $\times 200$ objective to determine the vascular density.

Tumor transplantation model. Female C57BL/6 mice, 4-week-old, were divided into four groups ($n = 6$): a pC-FGF-, a pC-Cyr-, and a pC-FGF/Cyr-treated group, and a control group. After anesthesia, vectors

(50 µg) were injected in tibialis anterior muscle followed by electrotransfer as described.⁸ Seven days later, mice were subjected to a subcutaneous injection of B16F0 cells in 100 µl phosphate-buffered saline in the right flank.

Tumor growth was monitored three times a week with a caliper 7 days after B16F0 cell implantation. Tumor volume was calculated with the formula: $V = Dd^2 \times 0.52$, where V is volume, D is maximum tumor diameter, and d is diameter at 90° to D . When tumors reached a size $>2,000 \text{ mm}^3$, mice were euthanized, and tumors were excised and weighed.

Statistical analysis. All statistical determination was performed with GraphPad Prism, version 4.0 (GraphPad, San Diego, CA). All data are presented as the mean \pm SEM. One-way and two-way analysis of variance was used to evaluate the significance of differences between groups. In some cases, data were analyzed using the post hoc Student's t -test for unpaired data and Bonferroni's correction for multiple comparisons. A P value of <0.05 was considered statistically significant.

SUPPLEMENTARY MATERIAL

Figure S1. Expression of mono- and bicistronic vectors in COS-7 cells.

Figure S2. Expression of Cyr61 and FGF2 proteins by mono- and bicistronic vectors in tibialis anterior muscle.

Figure S3. Protein and RNA expression of mono- and bicistronic vectors in C2C12 myoblasts.

Figure S4. Angiographic analysis of collateral vessel development in the ischemic limb treated by vector pC-FGF1Cyr or pC-RiCyr.

Materials and Methods.

ACKNOWLEDGMENTS

We thank Pascal Clerc and Hervé Prats for helpful discussions and Jason Iacovoni for proofreading. We also thank Yara Barreira, Sophie Legonidec, and Christine Fourreau (IFR150 animal functional exploration facility) and Jean-José Maoret (IFR150 quantitative transcriptomics facility), as well as Nadéra Ainaoui, Amar Deelchand, Sophie Dehez, Marie-José Fouque, and Fanny Sage for technical assistance. We thank the IFR150 BIVIC vector production facility (coordinators Loïc Van Den Berghe, Fabian Gross). This work was supported by grants from Fondation de l'Avenir, Agence Nationale pour la Recherche, Association Française contre les Myopathies, Association pour la Recherche sur le Cancer, Ligue Contre le Cancer, and Conseil Régional Midi-Pyrénées. A.R. has a fellowship from Association pour la Recherche sur le Cancer.

REFERENCES

- Criqui, MH (2005). Obesity, risk factors, and predicting cardiovascular events. *Circulation* **111**: 1869–1870.
- Al Sabti, H (2007). Therapeutic angiogenesis in cardiovascular disease. *J Cardiothorac Surg* **2**: 49.
- Ylä-Herttuala, S and Alitalo, K (2003). Gene transfer as a tool to induce therapeutic vascular growth. *Nat Med* **9**: 694–701.
- Bobek, V, Taltynov, O, Pinterova, D and Kolostova, K (2006). Gene therapy of the ischemic lower limb—Therapeutic angiogenesis. *Vascul Pharmacol* **44**: 395–405.
- Isner, JM, Pieczek, A, Schainfeld, R, Blair, R, Haley, L, Asahara, T *et al.* (1996). Clinical evidence of angiogenesis after arterial gene transfer of phVEGF165 in patient with ischaemic limb. *Lancet* **348**: 370–374.
- Nikol, S, Baumgartner, I, Van Belle, E, Diehm, C, Visoná, A, Capogrossi, MC *et al.* (2008). Therapeutic angiogenesis with intramuscular NV1FGF improves amputation-free survival in patients with critical limb ischemia. *Mol Ther* **16**: 972–978.
- Grundmann, S, Piek, JJ, Pasterkamp, G and Hoefler, IE (2007). Arteriogenesis: basic mechanisms and therapeutic stimulation. *Eur J Clin Invest* **37**: 755–766.
- Allera-Moreau, C, Delluc-Clavières, A, Castano, C, Van den Berghe, L, Golzio, M, Moreau, M *et al.* (2007). Long term expression of bicistronic vector driven by the FGF-1 IRES in mouse muscle. *BMC Biotechnol* **7**: 74.
- Vagner, S, Galy, B and Pyronnet, S (2001). Irresistible IRES. Attracting the translation machinery to internal ribosome entry sites. *EMBO Rep* **2**: 893–898.
- Delluc-Clavières, A, Le Bec, C, Van den Berghe, L, Conte, C, Allo, V, Danos, O *et al.* (2008). Efficient gene transfer in skeletal muscle with AAV-derived bicistronic vector using the FGF-1 IRES. *Gene Ther* **15**: 1090–1098.
- Couffignal, T, Silver, M, Kearney, M, Sullivan, A, Witzchenbichler, B, Magner, M *et al.* (1999). Impaired collateral vessel development associated with reduced expression of vascular endothelial growth factor in ApoE^{-/-} mice. *Circulation* **99**: 3188–3198.
- Fataccioli, V, Abergel, V, Wingertsmann, L, Neuville, P, Spitz, E, Adnot, S *et al.* (2002). Stimulation of angiogenesis by Cyr61 gene: a new therapeutic candidate. *Hum Gene Ther* **13**: 1461–1470.
- Babic, AM, Kireeva, ML, Kolesnikova, TV and Lau, LF (1998). Cyr61, a product of a growth factor-inducible immediate early gene, promotes angiogenesis and tumor growth. *Proc Natl Acad Sci USA* **95**: 6355–6360.
- Kireeva, ML, MO, FE, Yang, GP and Lau, LF (1996). Cyr61, a product of a growth factor-inducible immediate-early gene, promotes cell proliferation, migration, and adhesion. *Mol Cell Biol* **16**: 1326–1334.
- Kolesnikova, TV and Lau, LF (1998). Human Cyr61-mediated enhancement of bFGF-induced DNA synthesis in human umbilical vein endothelial cells. *Oncogene* **16**: 747–754.
- Kang, J, Albadawi, H, Patel, VI, Abbruzzese, TA, Yoo, JH, Austen, WG *et al.* (2008). Apolipoprotein E^{-/-} mice have delayed skeletal muscle healing after hind limb ischemia-reperfusion. *J Vasc Surg* **48**: 701–708.
- Cao, R, Bråkenhielm, E, Pawliuk, R, Wariaro, D, Post, MJ, Wahlberg, E *et al.* (2003). Angiogenic synergism, vascular stability and improvement of hind-limb ischemia by a combination of PDGF-BB and FGF-2. *Nat Med* **9**: 604–613.
- Chae, JK, Kim, I, Lim, ST, Chung, MJ, Kim, WH, Kim, HG *et al.* (2000). Coadministration of angiotensin-1 and vascular endothelial growth factor enhances collateral vascularization. *Arterioscler Thromb Vasc Biol* **20**: 2573–2578.
- Lee, JS, Kim, JM, Kim, KL, Jang, HS, Shin, IS, Jeon, ES *et al.* (2007). Combined administration of naked DNA vectors encoding VEGF and bFGF enhances tissue perfusion and arteriogenesis in ischemic hindlimb. *Biochem Biophys Res Commun* **360**: 752–758.
- Jünemann, C, Song, Y, Bassili, G, Goergen, D, Henke, J and Niepmann, M (2007). Picornavirus internal ribosome entry site elements can stimulate translation of upstream genes. *J Biol Chem* **282**: 132–141.
- Bornes, S, Prado-Lourenco, L, Bastide, A, Zanibellato, C, Iacovoni, JS, Lacazette, E *et al.* (2007). Translational induction of VEGF internal ribosome entry site elements during the early response to ischemic stress. *Circ Res* **100**: 305–308.
- Conte, C, Riant, E, Toutain, C, Pujol, F, Arnal, JF, Lenfant, F *et al.* (2008). FGF2 translationally induced by hypoxia is involved in negative and positive feedback loops with HIF-1 α . *PLoS ONE* **3**: e3078.
- Zhang, SH, Reddick, RL, Piedrahita, JA and Maeda, N (1992). Spontaneous hypercholesterolemia and arterial lesions in mice lacking apolipoprotein E. *Science* **258**: 468–471.
- Martineau, Y, Le Bec, C, Monbrun, L, Allo, V, Chiu, IM, Danos, O *et al.* (2004). Internal ribosome entry site structural motifs conserved among mammalian fibroblast growth factor 1 alternatively spliced mRNAs. *Mol Cell Biol* **24**: 7622–7635.



This work is licensed under the Creative Commons Attribution-NonCommercial-No Derivative Works 3.0 License. To view a copy of this license, visit <http://creativecommons.org/licenses/by-nc-nd/3.0/>